ENGLE

AFML-TR-72-163

FATIGUE CRACK GROWTH RETARDATION AFTER SINGLE-CYCLE PEAK OVERLOAD IN Ti-6 A1-4V TITANIUM ALLOY

R. E. JONES

UNIVERSITY OF DAYTON
RESEARCH INSTITUTE

TECHNICAL REPORT AFML-TR-72-163

APRIL 1972

20071126018

AIR FORCE MATERIALS LABORATORY
AIR FORCE SYSTEMS COMMAND
WRIGHT-PATTERSON AIR FORCE BASE, OHIO

NOTICE

When Government drawings, specifications, or other data are used
other than in connection with a definitely related Government procurement
operation, the United States Government thereby incurs no responsibility
nor any obligation whatsoever; and the fact that the government may
have formulated, furnished, or in any way supplied the said drawings,
specifications, or other data, is not to be regarded by implication or
otherwise as in any manner licensing the holder or any other person or
corporation, or conveying any rights or permission to manufacture, use,
or sell any patented invention that may in any way be related thereto.

FATIGUE CRACK GROWTH RETARDATION AFTER SINGLE-CYCLE PEAK OVERLOAD IN Ti-6 A1-4V TITANIUM ALLOY

R. E. JONES

Approved for public release; distribution unlimited.

FOREWARD

This report was prepared by the University of Dayton Research Institute, Dayton, Ohio. The work was performed under USAF Contract No. F33615-71-C-1054. The contract was initiated under Project No. 7381, "Materials Applications," Task No. 738106, "Design Information Development," and administered by the Air Force Materials Laboratory, Wright-Patterson Air Force Base, Ohio, Mr. David C. Watson (AFML/LAE), Project Engineer.

All (or many) of the items compared in this report were commercial items that were not developed or manufactured to meet Government specifications, to withstand the tests to which they were subjected, or to operate as applied during this study. Any failure to meet the objectives of this study is no reflection on any of the commercial items discussed herein or on any manufacturer.

The author would like to acknowledge that testing performed for this program was accomplished by Messrs. Lawrence Sears and J. H. Eblin. Engineering support was provided by Mr. G. J. Petrak.

The report covers work conducted from April 1971 to December 1971.

The report was submitted by the author in May 1972.

This technical report has been reviewed and is approved.

A. OLEVITCH
Chief, Materials Engineering Branch
Materials Support Division
Air Force Materials Laboratory

ABSTRACT

Fatigue crack growth after single-cycle peak overload was investigated in Ti-6Al-4V sheet. Strain hardening was determined not to be the major controlling mechanism retarding crack growth after peak overload, but instead, strain hardening slightly accelerated carck growth for the case when strain hardening was induced prior to crack initiation. Crack growth after peak overload was characterized by: (1) no effect after 20 percent overload (a 20 percent increase in maximum stress intensity); (2) crack arrest immediately following 70 and 100 percent overloads; (3) subsequent retarded crack growth rates after 70 and 100 percent overloads; and (4) retardation but no arrest following 50 percent overload. The Wheeler model of crack growth retardation was discussed and shown not to predict instantaneous retarded growth rates. The physical appearance of post-test fracture surfaces were as hypothesized by the Elber concept of crack closure after overload. The recovery of an overloaded crack was linear with respect to the constant load amplitude cyclic stress intensity.

TABLE OF CONTENTS

LIST OF FIGURES

LIST OF TABLES

NOMENCLATURE

a	half crack length as measured from specimen centerline to crack tip
a_n	current crack length utilized in Wheeler formula
a_o	original crack length utilized in Wheeler formula
a_p	current crack length plus the radius of the largest previous yield zone
C	material constant determined from constant load amplitude crack growth data (constant utilized in Paris crack growth equation)
C_P	Wheeler retardation parameter
da/dN	instantaneous crack growth per cycle
$(da/dN)_{C.A.}$	instantaneous constant load amplitude crack growth rate occurring at same crack length as $da/dN_{O.L.}$ but under constant amplitude loading conditions
$(da/dN)_{O.L.}$	instantaneous retarded crack growth rate following single-cycle overload
$f(\Delta K_I)$	function of cyclic stress intensity
F_W	Isida finite width correction
$K_{C.A.}$	maximum stress intensity occurring in constant load amplitude cycle prior to overload
K_I	linear elastic plane strain stress intensity
$K_{O.L.}$	maximum stress intensity during overload cycle
m	data correlating exponent for Wheeler formula
n	data fitting exponent determined from constant load amplitude crack growth data (constant utilized in Paris crack growth equation)
$O.L.$	overload
q	slope of linear relationship between Z and $\Delta K_{C.A.}$
R	minimum fatigue load divided by maximum fatigue load
R_y	radius of current yield zone

NOMENCLATURE, continued

r_y	plane strain yield zone radius
U	Elber effective stress ratio
W	width of specimen at the test section
Z	recovery factor
Z_i, $(\Delta K_{C.A.})_i$	any simultaneous recovery factor and cyclic constant load amplitude stress intensity, respectively, under the influence of an overload
Z_o	intercept of ordinate if $\Delta K_{C.A.} = 0$ when considering linear relationship between Z and $\Delta K_{C.A.}$
ΔK_I	cyclic stress intensity
$\Delta K\,eff$	effective cyclic stress intensity factor utilized in Elber model
Δr_y	relative cyclic plastic zone radius
σ	gross stress
σ_{max}	maximum applied stress
σ_{min}	minimum applied stress
σ_{OP}	stress at which crack tip opens
$\sigma_{y.s.}$	yield stress

INTRODUCTION

The use of high strength materials in modern military aircraft has become necessary in order to increase aircraft performance capabilities. However, these materials have presented several problems not confronted with medium and low strength material structures. One problem which is of major concern is the sensitivity of high strength materials to flaws or defects. When these materials are loaded, flaws become a source of propagating cracks and subsequent catastrophic component failure.

The visual detection and arrest of subcritical cracks has been possible in many cases. However, when cracks stem from internal material flaws or propagate in areas which are not accessible without a major aircraft disassembly, their detection and repair before reaching critical dimensions is physically impossible. It is therefore necessary that an analysis of crack growth in high strength aircraft materials be made available so as to confidently predict when to accomplish some repair, component replacement, or to remove aircraft from service. This prediction of component or aircraft life would be based on the maximum material flaw size allowable at the time of material fabrication.

In an effort to obtain useful and workable analyses of crack growth, researchers (References 1 and 2) have investigated the effect of constant amplitude loading on propagating fatigue cracks. Empirical relationships have been developed by several investigators for the case of constant amplitude loading, utilizing a linear elastic stress intensity (K_I) approach. The main premise of these relationships has been that the crack growth rate (da/dN) resulting from a constant load amplitude

1

is a function of the change in stress intensity (ΔK_I) at the crack tip during load cycling. The general form of the developed equations is $da/dN = f(\Delta K_I)$. The two most notable of these equations are as follows:

$$da/dN = C(\Delta K_I)^n \qquad \text{Paris Equation}$$

$$da/dN = \frac{C(\Delta K_I)^n}{(1-R)K_c - \Delta K_I} \qquad \text{Forman Equation}$$

With these simplified versions of crack growth as a base, the effects of other influences must also be analyzed for an accurate prediction of aircraft life. One such influence involves the retarding effect of peak overloads on subsequent crack growth. When the retarding effect of peak overload on crack growth is disregarded, the prediction of material life is usually very conservative. For more accurate predictions of the cyclic life to failure, peak overload mechanisms must be understood and mathematically modeled.

To date only a few investigators have studied the retarding effects of peak overload on crack growth. These researchers have proposed several mechanisms in an attempt to explain the retardation phenomenon. Among these proposed mechanisms are: (1) compressive residual stresses at the crack tip (Reference 3); (2) change in geometrical shape of the crack tip (Reference 4); (3) crack closure (Reference 5); and (4) yield zone interaction (Reference 6). Of the hypothetical mechanisms introduced, none as yet has been conclusively shown to be the prime influence on crack growth after overload. However, several of these mechanisms have been successfully used to empirically model retarded crack growth behavior.

Another conceivable factor in crack retardation which has not been previously considered is strain hardening. Crack tip strain

hardening (cold working) is the progressive strengthening of the region in the vicinity of a crack tip due to excessively high plastic straining or permanent cold working deformation. This paper demonstrates that strain hardening is not a mechanism of fatigue crack growth retardation after peak overload. The study is accomplished by comparing crack growth rates among a series of specimens having different prestrain levels with cracking rates in unstrained material.

In addition to strain hardening, other mechanisms such as yield zone interaction and crack closure are studied and evaluated. The Wheeler and Elber retardation models which consider yield zone interaction and crack closure, respectively, are discussed. A considerable portion of the report concentrates on the development of a retardation model based on the test findings.

It must be realized that this is an exploratory study of crack growth retardation after peak overload, and that conclusive proof will not be contained in this report.

MATERIAL AND SPECIMENS

An annealed Ti-6Al-4V sheet measuring 96 inches by 36 inches by 0.063 inches was received from TMCA (Titanium Metals Corporation of America) for testing purposes. The sheet was heat treated according to MIL T 9046F specifications. The chemical composition of the sheet which is presented in Table I was certified by TMCA.

TABLE I

Chemical Analysis of Ti-6Al-4V Test Sheet

Chemical Composition (% by weight)						
C	Fe	N	Al	V	H	O
0.026	0.09	0.011	5.8	3.8	0.008	0.14

Tensile specimens were machined from the center section of the sheet in both the longitudinal (length) and the transverse (width) directions. Three specimens were removed from each direction. The tensile specimen configuration is shown in Figure 1.

Center notched specimens for crack growth testing were machined in the longitudinal direction of the sheet. Loading was parallel to the longitudinal grain structure while crack growth was in the transverse direction of the sheet. The center notched specimen configuration is presented in Figure 2. Cracks were initiated from the starter notch shown in the detail of Figure 2 by fatigue loading. All but two specimens were removed from a 7 foot by 1 foot strip taken from an edge section of the test sheet. Ten crack growth specimens were machined from the sheet. Two specimens were tested with constant load amplitude parameters, five were tested with strain hardening/constant load amplitude conditions, and three were tested with peak overload/constant load amplitude conditions.
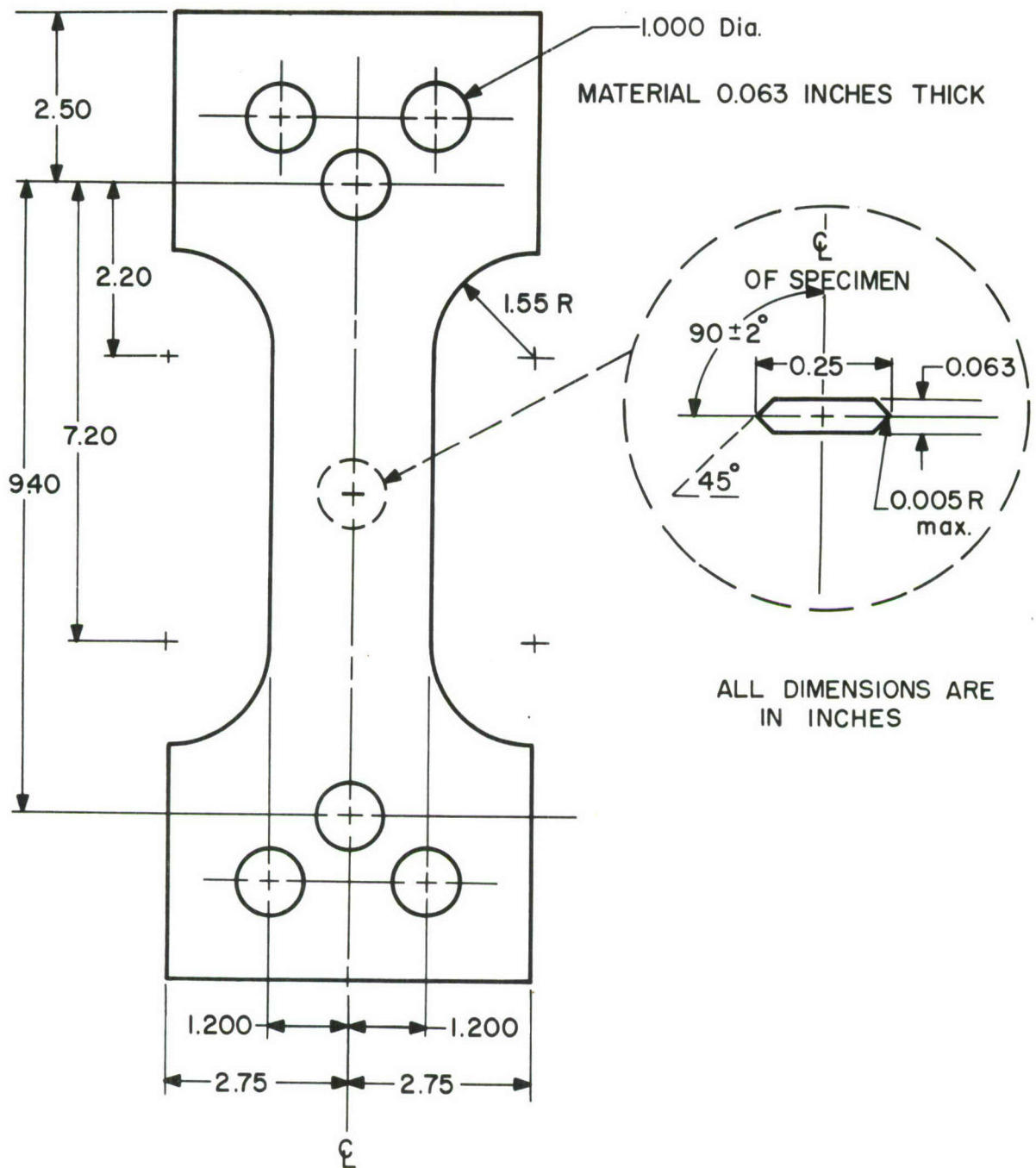
4

Figure 1. Tension Specimen Configuration

MATERIAL 0.063 INCHES THICK

ALL DIMENSIONS ARE IN INCHES

0.250

¢

0.250

1.00

1.50

5.50

4.00

2.000
GAGE LENGTH

1.000 R

0.500 DIA.

0.75

0.75

5

Figure 2. Crack Growth Specimen Configuration

TEST PROCEDURES

Tensile testing was performed according to the ASTM (American Society for Testing and Materials) standard testing procedures utilizing a Wiedemann Tensile Testing Machine.

Crack growth testing was performed with an MTS Systems Corporation closed-loop hydraulic fatigue testing system. A sinusoidal loading wave form and a loading frequency of 60 cpm were utilized for all crack growth testing with an exception being that peak overloads were applied at 10 cpm. A maximum load of 3000 lbs and an "R" ratio (minimum fatigue load to maximum fatigue load) of 0.1 were also used for every crack growth test, with the only exception being that the maximum load was changed with peak overload applications. Crack lengths were measured from tip to tip with a 10X Gaertner traveling microscope (see Figure 3). Cracks grew symmetrically in the test specimens as occasional checks showed equal crack lengths on both sides of the specimen's centerline.

The three types of crack growth testing were performed as follows:

(1) Constant Load Amplitude

Fatigue cracks were propagated in the "as-received" material. The loading amplitude, mean load, and frequency were maintained constant throughout the entire test.

(2) Strain Hardening/Constant Load Amplitude

Unnotched specimens were deformed in tension to various percentages of plastic strain. The plastic straining prior to crack growth testing was performed in the Wiedemann Tensile Testing Machine with a resistive bridge extensometer used as a strain monitor. The
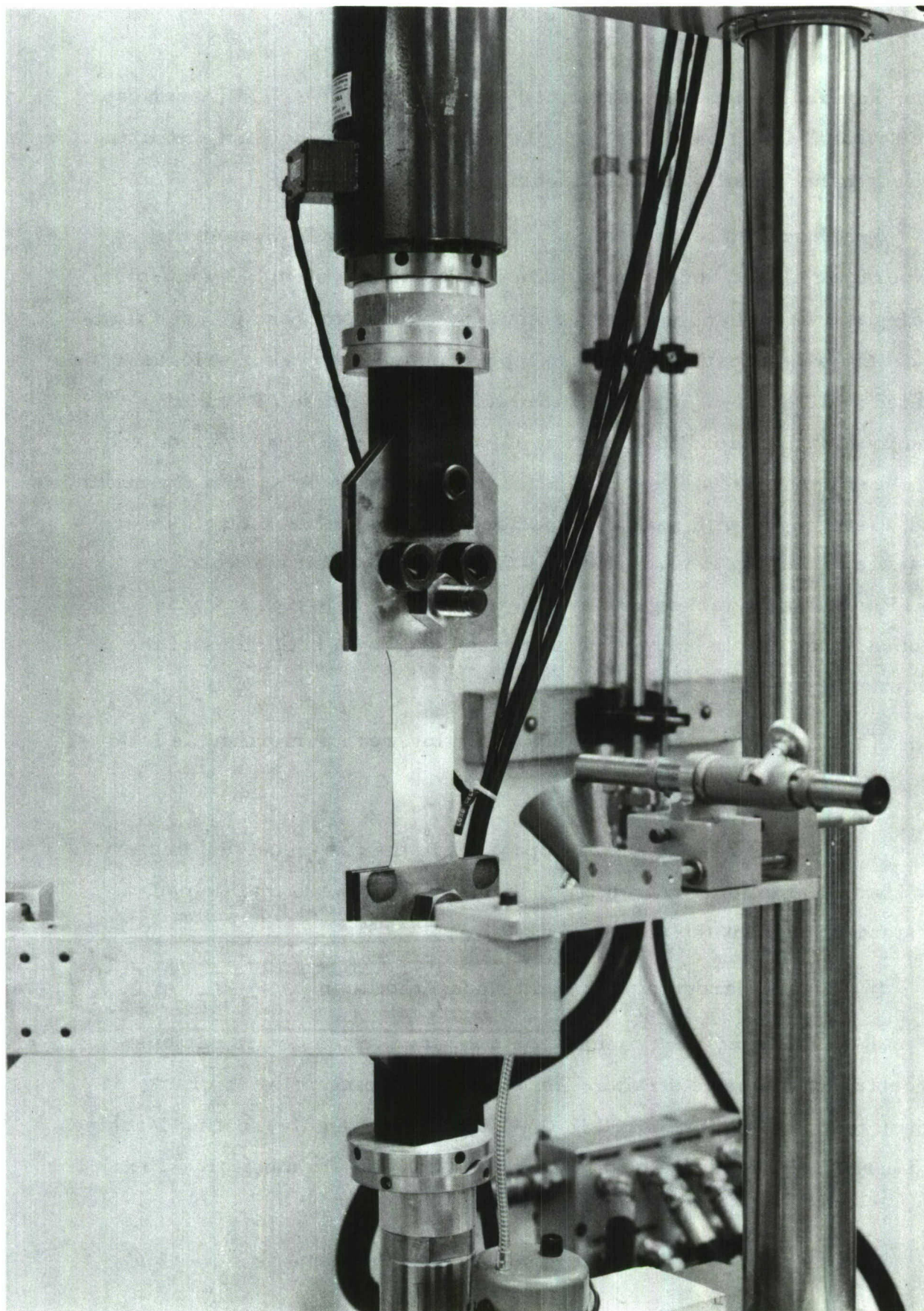
Figure 3. Test Arrangement for Center Notched Crack Growth Specimens

8

extensometer measured strain on the centerline of both faces of the specimens indicating an average strain on a load versus strain plot. Specimens were prestrained to 2.41%, 3.85%, 6.10%, 7.00%, and 10.00% plastic strain. These values of plastic strain were determined from the load versus strain plots by measuring from the 0.2% offset strain to the strain at which the load was removed. This plastic deformation was intended to simulate the extreme yielding at the crack tip during overload. Center notches were then machined into the specimens and fatigue cracks propagated utilizing constant amplitude loading parameters.

(3) Peak Overload/Constant Load Amplitude

Cracks were propagated in center notched specimens utilizing constant amplitude loading parameters prior to overload application. Peak overloads were applied such that the peak stress intensities reached during overload were 20%, 50%, 70%, and 100% greater than the maximum stress intensity just prior to overload application. The minimum load during peak overload was the same as that of a constant load amplitude test. There was a momentary pause at the minimum load before and after each overload application. This pause was not considered long enough to have an effect on subsequent crack growth. After overload, the same constant amplitude loading parameters were employed as those prior to overload.

Stretch zones associated with crack overload were measured at the center of the specimen thickness utilizing a scanning electron microscope.

9

RESULTS AND DISCUSSION

The tensile properties of the Ti-6Al-4V test sheet are presented in Table II.

TABLE II

Tensile Properties of Annealed Ti-6Al-4V Sheet

Direction		Ultimate Strength (KSI)	Yield Strength (KSI)	Elongation In 2 Inches (%)
Longitudinal		142.6	134.4	14.4
		142.9	133.6	13.3
		142.9	133.6	12.2
	Average	142.8	133.9	13.3
Transverse		141.6	137.2	13.4
		142.1	137.6	14.1
		142.1	137.9	12.3
	Average	141.9	137.6	13.3

Although the average ultimate strength and elongation were similar in the longitudinal and transverse directions of the sheet, the average yield strength was slightly higher in the transverse direction. Photo-micrographs were made parallel to the longitudinal, transverse, and short transverse directions of a center section of the test sheet to establish grain orientations. The photomicrographs showed that the microstructure was predominantly equiaxed with a slight tendency for long grains to be oriented in the longitudinal direction of the sheet (see Figure 4).

The observed crack length versus the number of fatigue cycles for each crack growth specimen is presented in Figures 5 through 14. Figures 5 and 6 present the constant load amplitude crack growth data for material containing no prestraining. Reviewing Figures 7 through

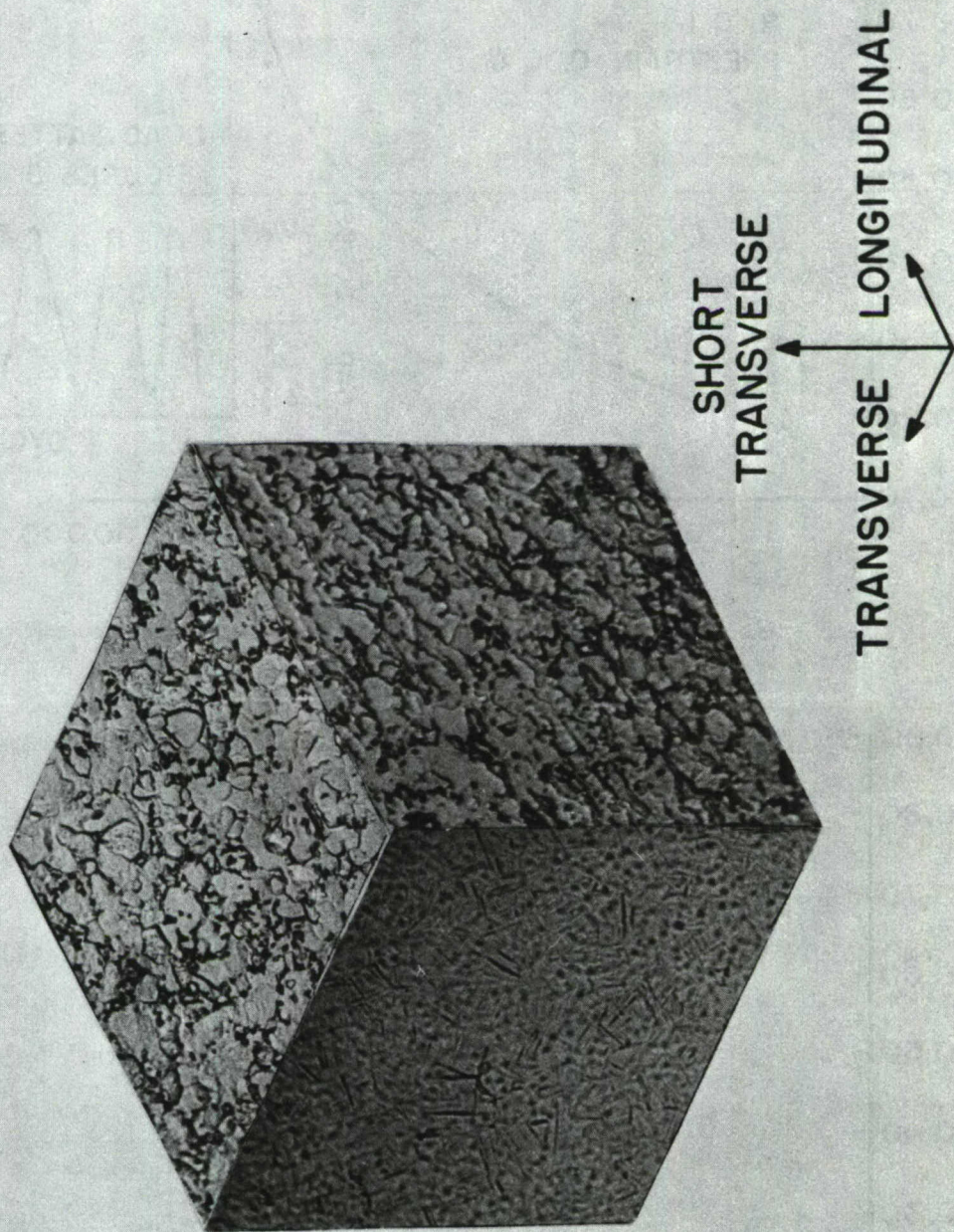Figure 4. Microstructure at Center Section of Annealed Ti-6Al-4V Sheet (500X)
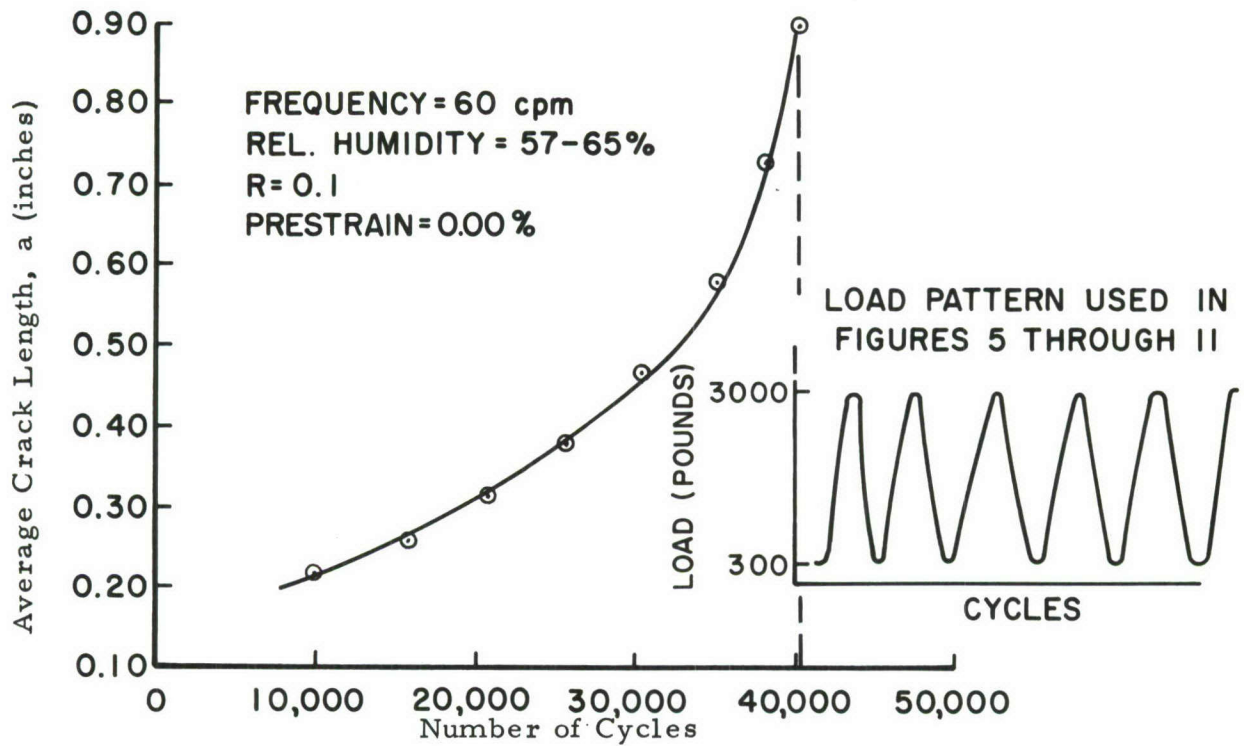
Figure 5. Constant Load Amplitude Crack Growth Curve (Specimen CG-10)
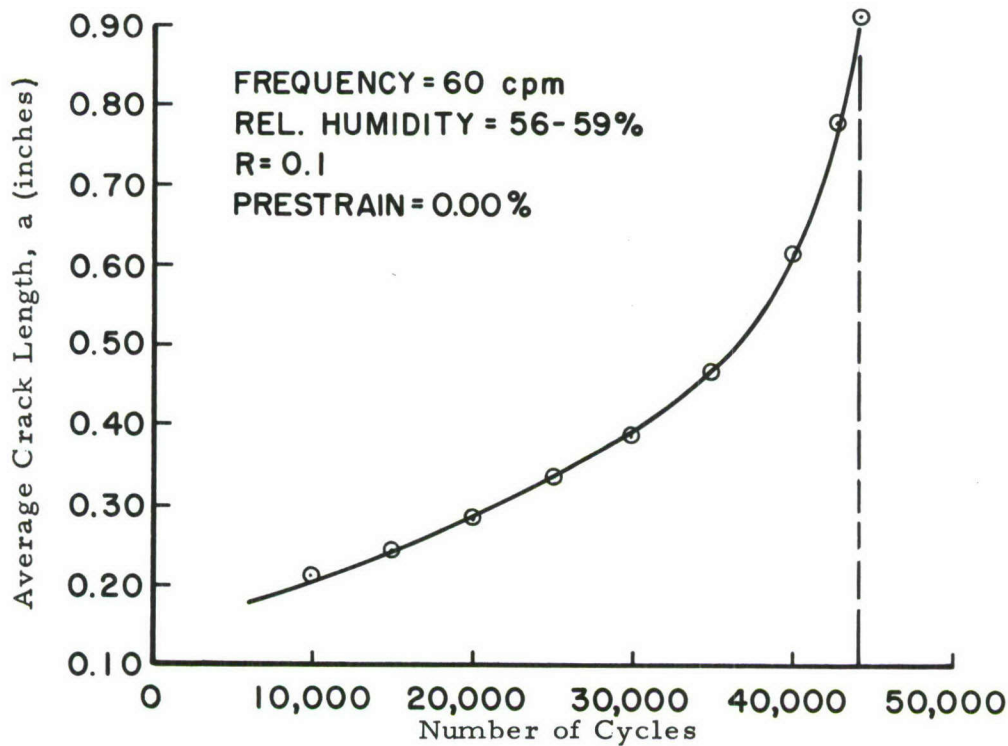
Figure 6. Constant Load Amplitude Crack Growth Curve (Specimen CG-6)

12

Figure 7. Constant Load Amplitude Crack Growth Curve for Strain Hardened Material (Specimen CG-2)

Figure 8. Constant Load Amplitude Crack Growth Curve for Strain Hardened Material (Specimen CG-8)

13

Figure 9. Constant Load Amplitude Crack Growth Curve for Strain
Hardened Material (Specimen CG-13)

Figure 10. Constant Load Amplitude Crack Growth Curve for Strain
Hardened Material (Specimen CG-5)

14
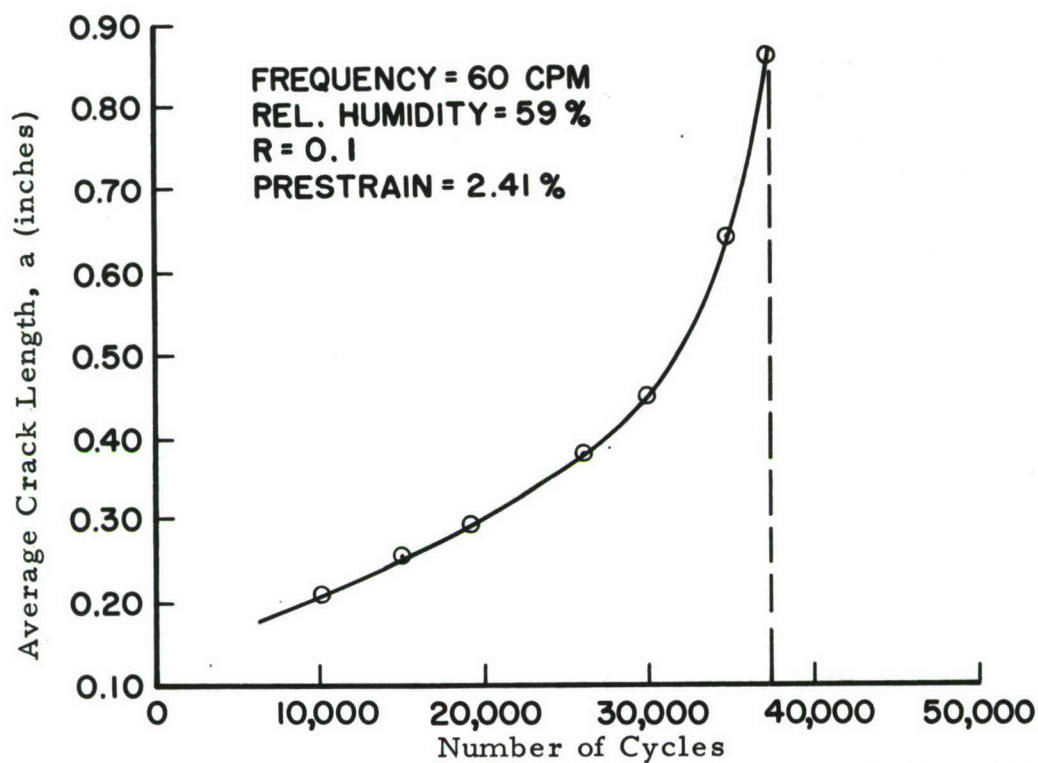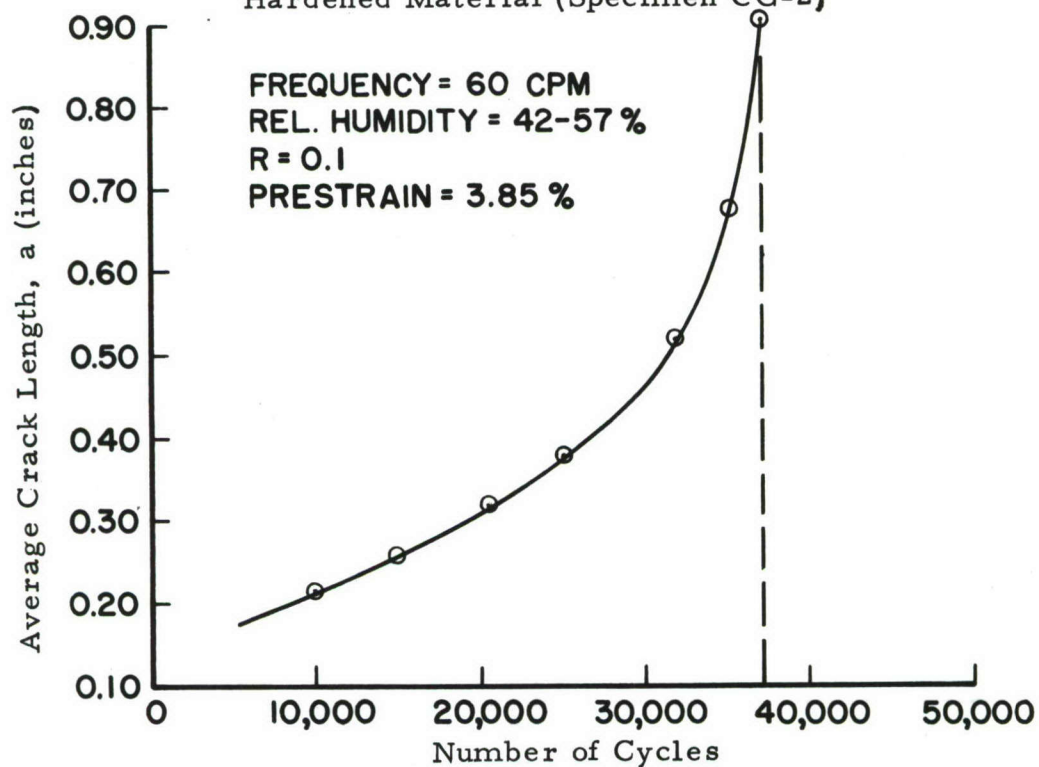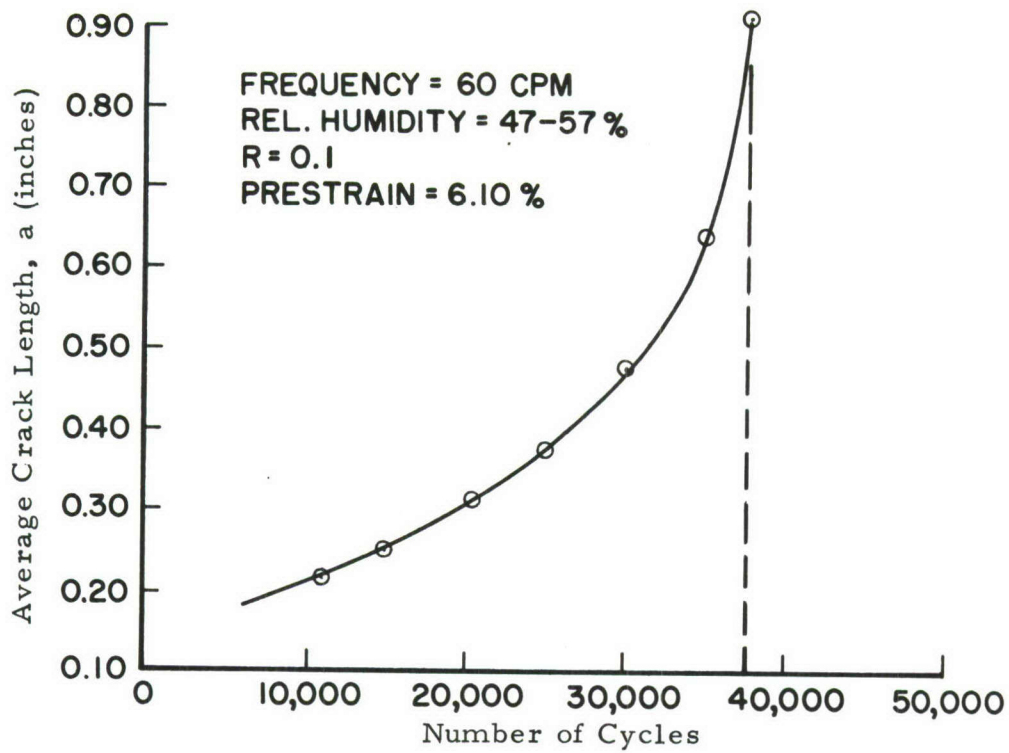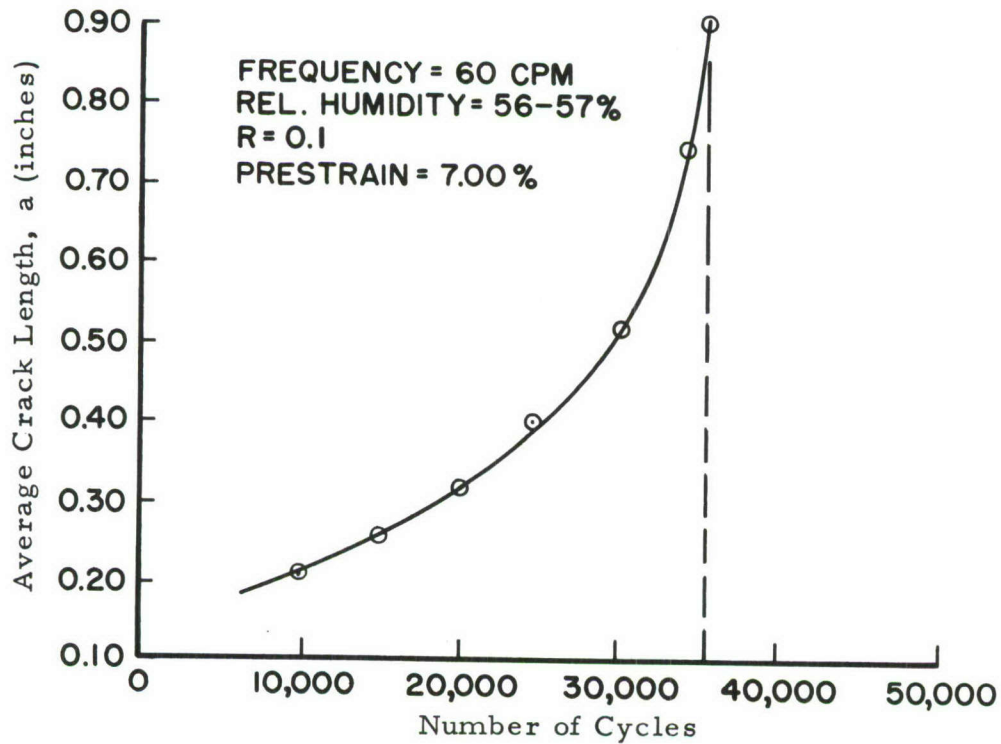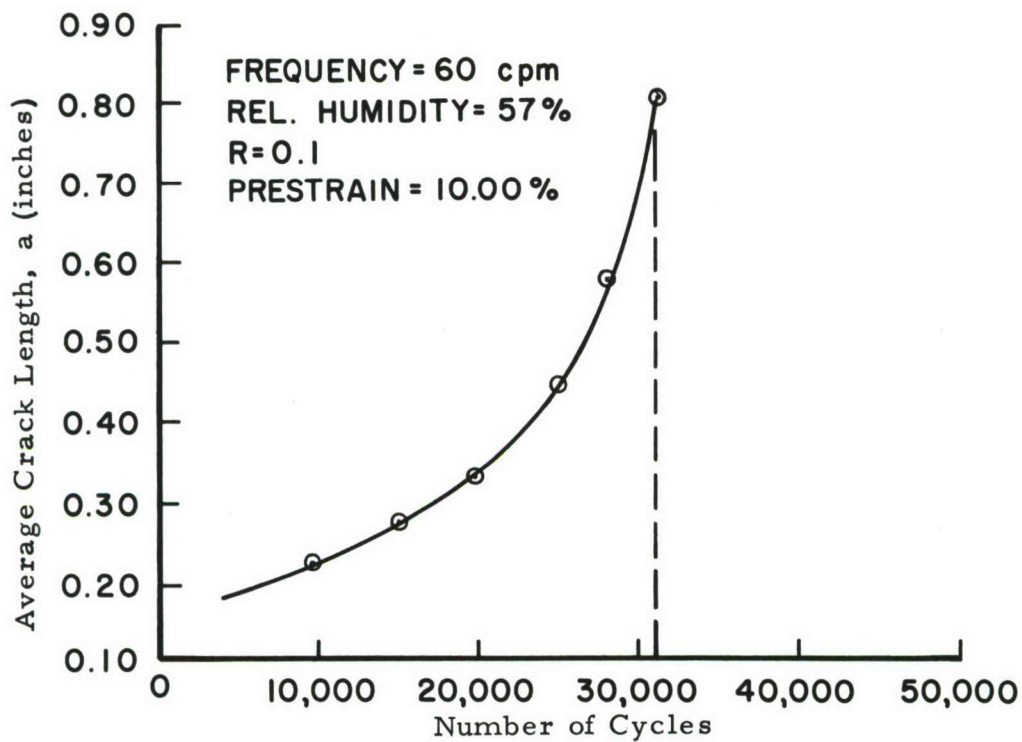
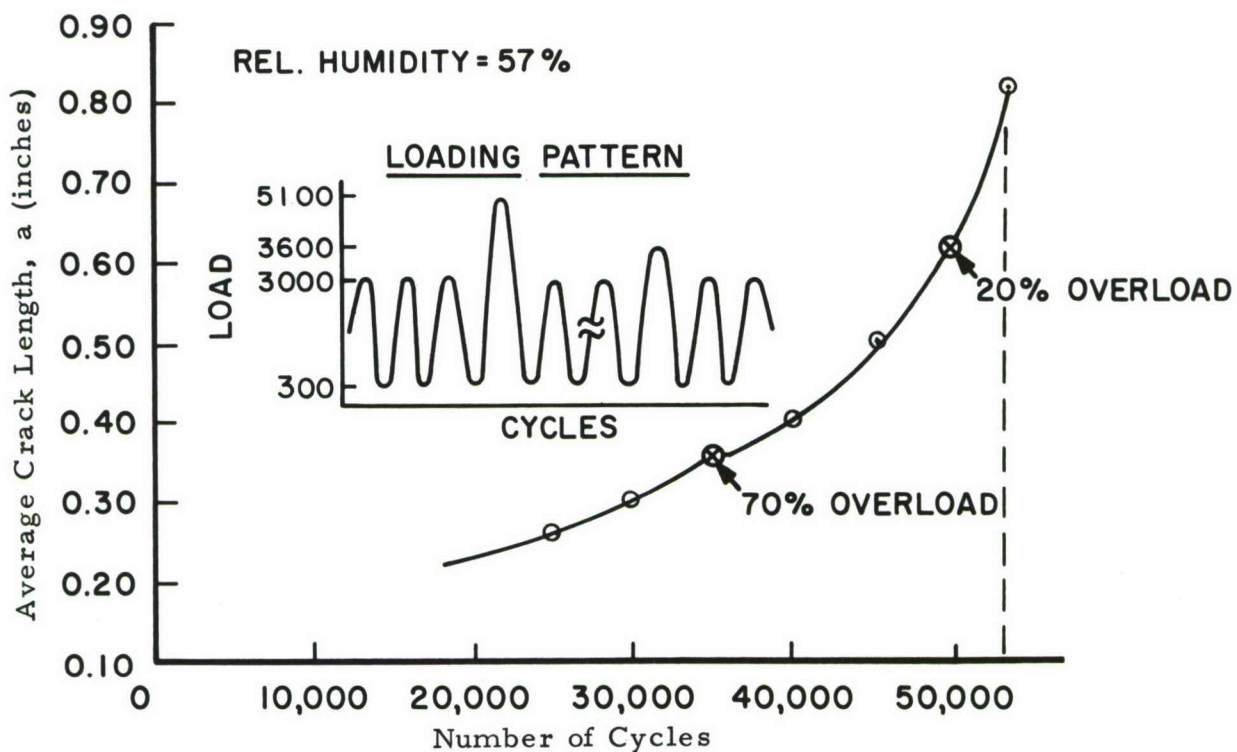Figure 11. Constant Load Amplitude Crack Growth Curve for Strain Hardened Material (Specimen CG-3)

Figure 12. Crack Growth Curve with 70% and 20% Single-Cycle Peak Overloads (Specimen CG-7)
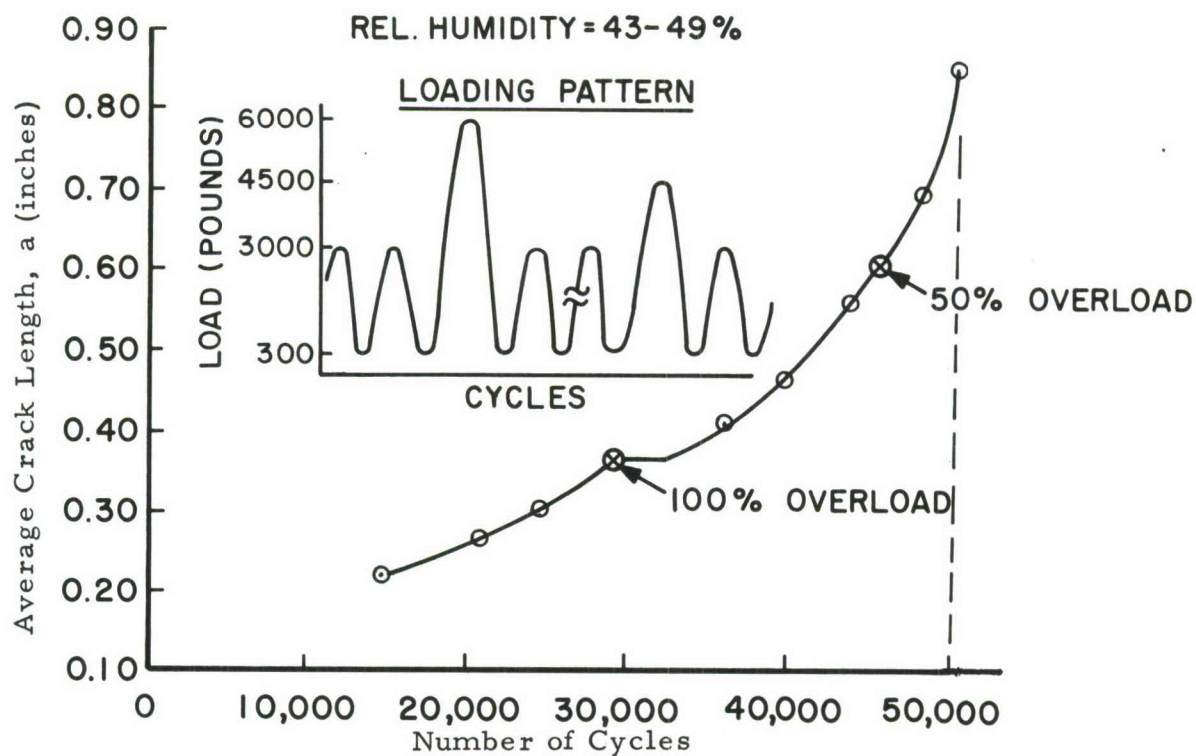
15

Figure 13. Crack Growth Curve with 100% and 50% Single-Cycle Peak Overloads (Specimen CG-1)
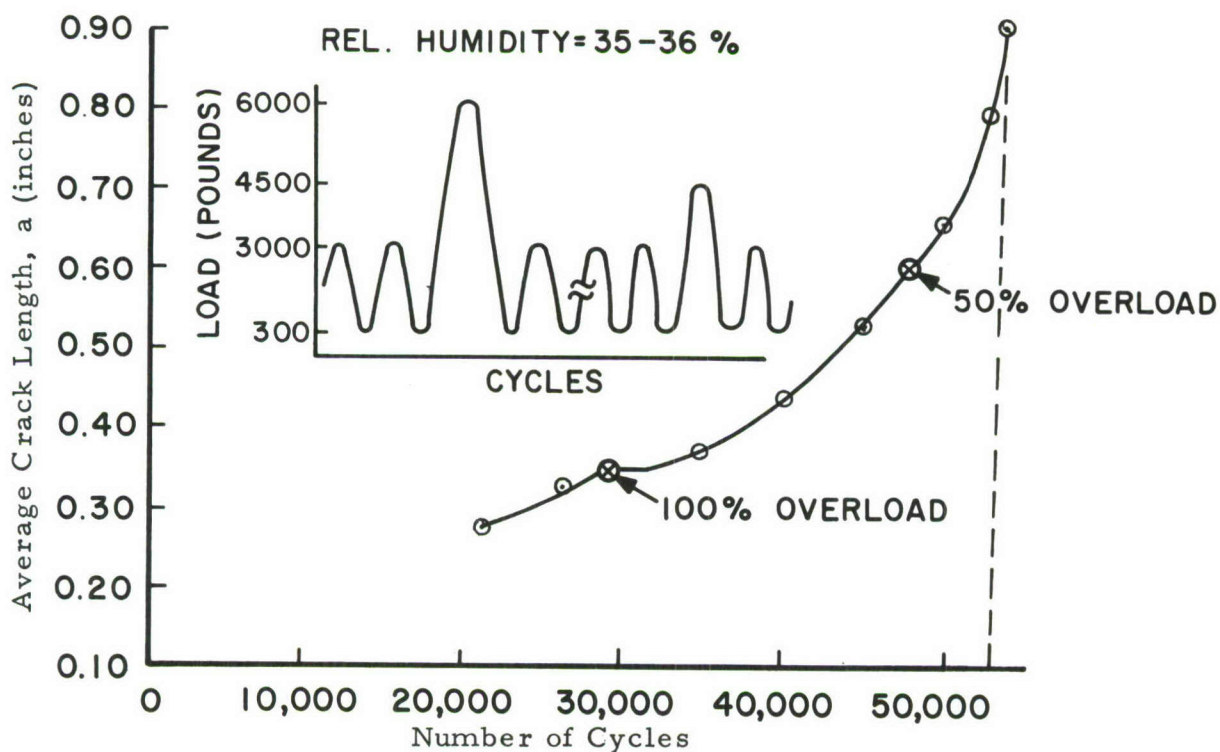

Figure 14. Crack Growth Curve with 100% and 50% Single-Cycle Peak Overloads (Specimen CG-14)

11, it can be seen that the strain hardened crack growth specimens have two interesting features. First, the cyclic life to failure is decreased substantially by hardening, and second, the net uncracked region just prior to specimen failure is approximately the same in each specimen. This indicates that the crack growth rate slightly accelerated with increasing hardening. Figures 12 through 14 show that the 50%, 70%, and 100% peak overloads definitely affected crack growth. Momentary pauses at the minimum load before and after peak overload applications are not depicted in the loading patterns of these figures, although pauses were necessary to manually change the load and frequency.

The constant load amplitude crack growth rate data obtained from two non-strain hardened center notched specimens is presented in Figure 15. It was concluded that two specimens were sufficient for baseline data since there was very little scatter in these data and they also compared favorably with data in the literature (Reference 9). The same loading parameters were used for generating baseline constant load amplitude crack growth data as were used for generating the pre-stained crack growth data and the constant load amplitude portion of the peak overload/constant load amplitude crack growth data.

Crack growth rate data obtained from the strain hardened specimens is presented in Figure 16. A search of the literature and the author's experience showed that annealed Ti-6Al-4V does strain harden. That is, there is an increase in yield strength and a decrease in ductility after cold working. Strain hardening slightly increased the fatigue crack growth rate from that growth rate obtained with annealed specimens. The original premise of this program was that the extreme plasticity produced at the crack tip by overload would be simulated by the plastic deformation due to strain hardening. But rather than the expected result of a retarded crack growth rate, the growth rate in the hardened
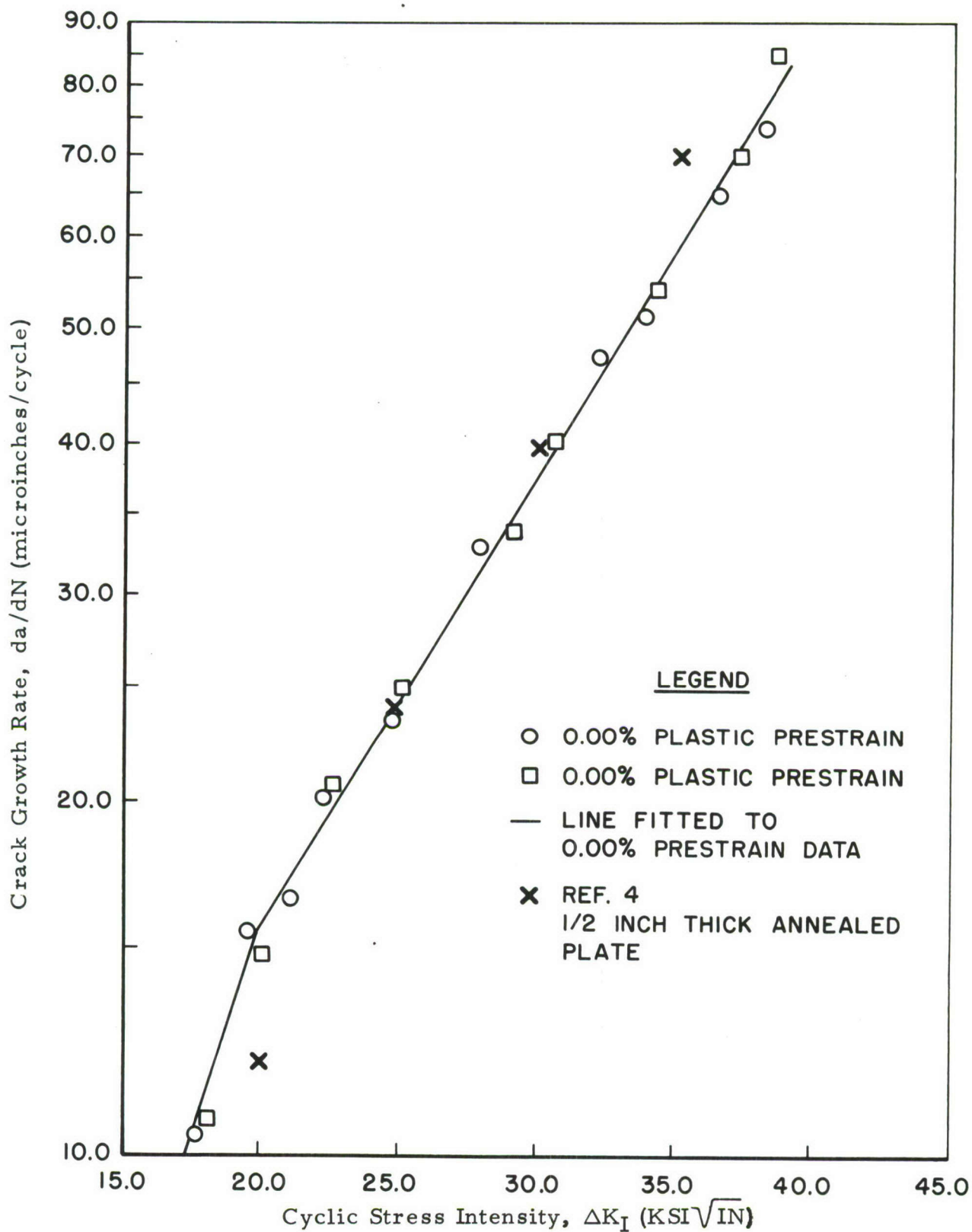
Figure 15. Crack Growth Rate Versus Cyclic Stress Intensity for Constant
Amplitude Crack Growth Data and Data from Reference 4
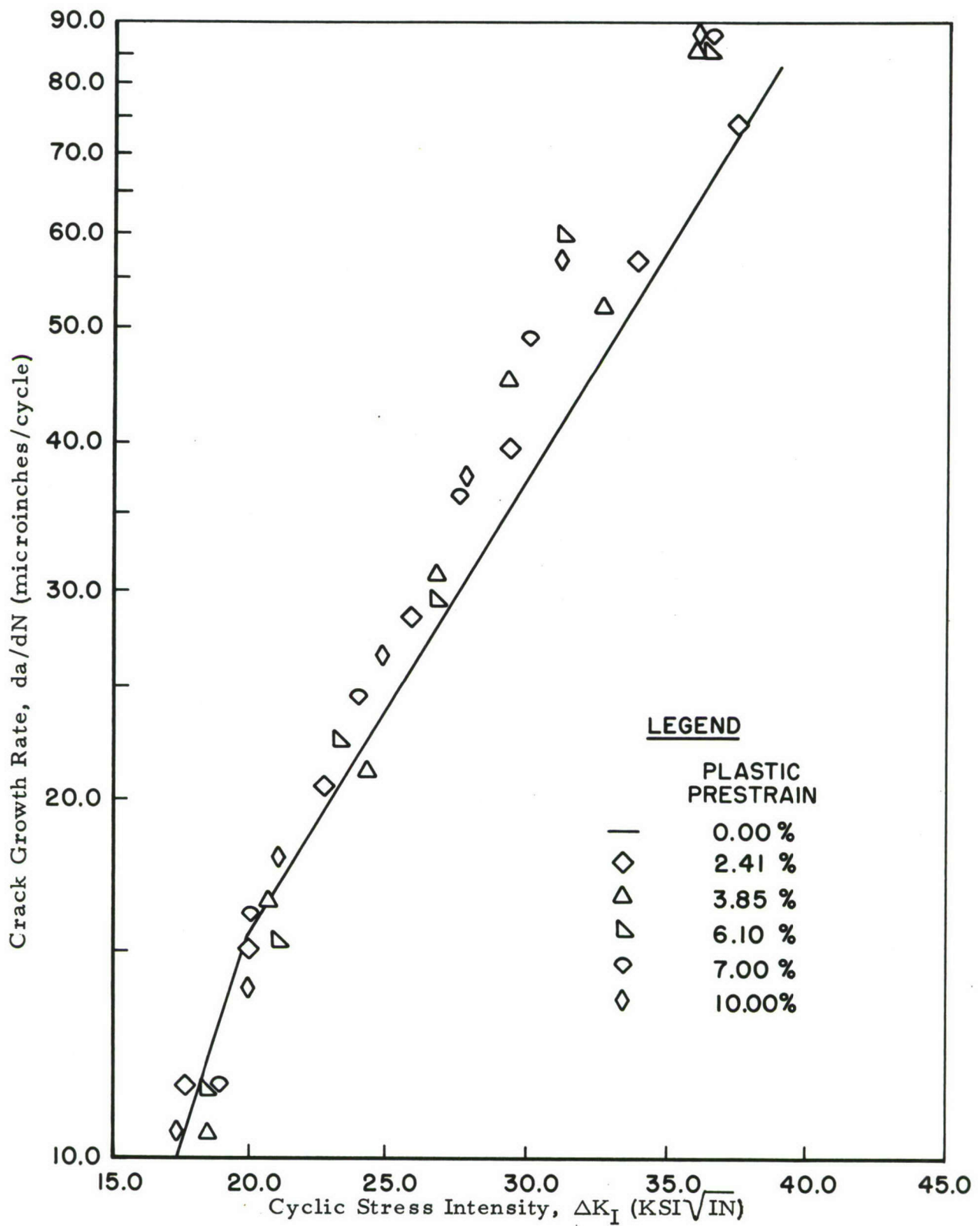(Specimens CG-10 and CG-6)

18

Figure 16. Crack Growth Rate Versus Cyclic Stress Intensity for Strain Hardened Material (Specimens CG-2, CG-8, CG-13, CG-15, and CG-3)

specimens was slightly accelerated. Therefore, rather than contributing to the retardation of growth rates after overload, the strain hardening mechanism slightly accelerates the cracking rate.

Peak overload/constant load amplitude cracking data is presented in Figures 17 through 19. The following results were observed: (1) a 20% peak overload had no apparent effect upon subsequent cracking behavior; (2) a 50% peak overload had a retarding effect upon the crack growth rate; however, there appeared to be continuous crack growth; (3) a 70% peak overload arrested the crack for approximately 1000 cycles and retarded the subsequent crack growth rate; and (4) a 100% peak overload arrested the crack for approximately 2100 to 2200 cycles and substantially retarded the fatigue cracking rate.

The crack length increments, arrested cycles, and the total number of cycles affected by the peak overloads are presented in Table III. These were the crack length increments and the number of cycles necessary for the overloaded crack to return to the cracking rate of a specimen with no peak overloads. These data were repeatable for the 100% and 50% peak overloads when testing duplicate specimens. The data tend to show that the percentage of overload may be used as an indicator of the amount of subsequent retardation.

The main concern of the remainder of this report will be the retardation effect of peak overload excluding crack arrest. Most of the analysis of retardation, to date, have used data fitting techniques in conjunction with the effective plastic zone or the effective crack opening (effective ΔK). Empirical relationships have been developed, the most notable of which are the Wheeler formula (Reference 6) and the Elber formula (Reference 5).

Wheeler's formula, which is concerned with the relationship of the current and previous yield zones at the crack tip, is as follows:
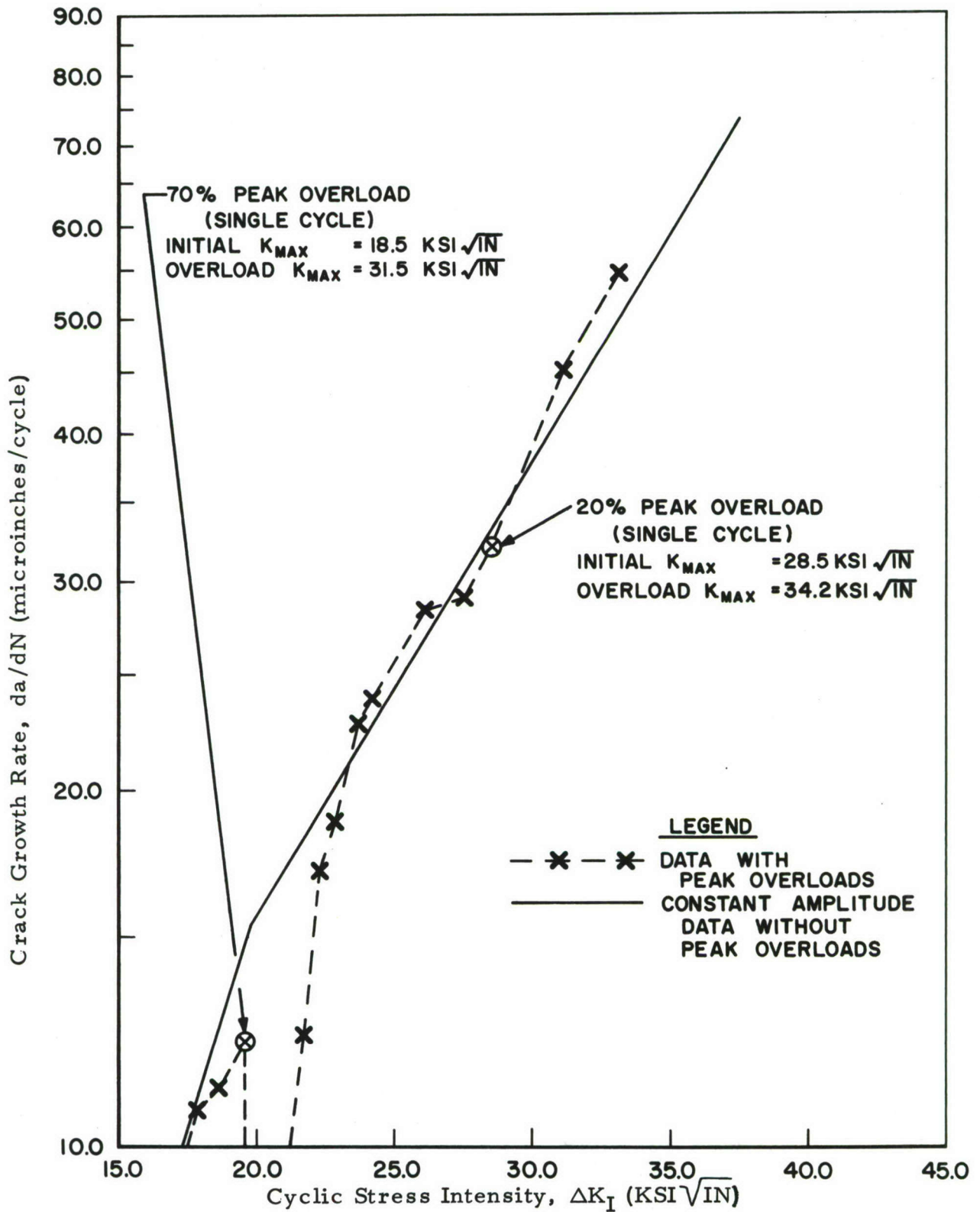
Figure 17. Crack Growth Rate Versus Cyclic Stress Intensity for 70% and 20% Single-Cycle Peak Overloads (Specimen CG-7)

21
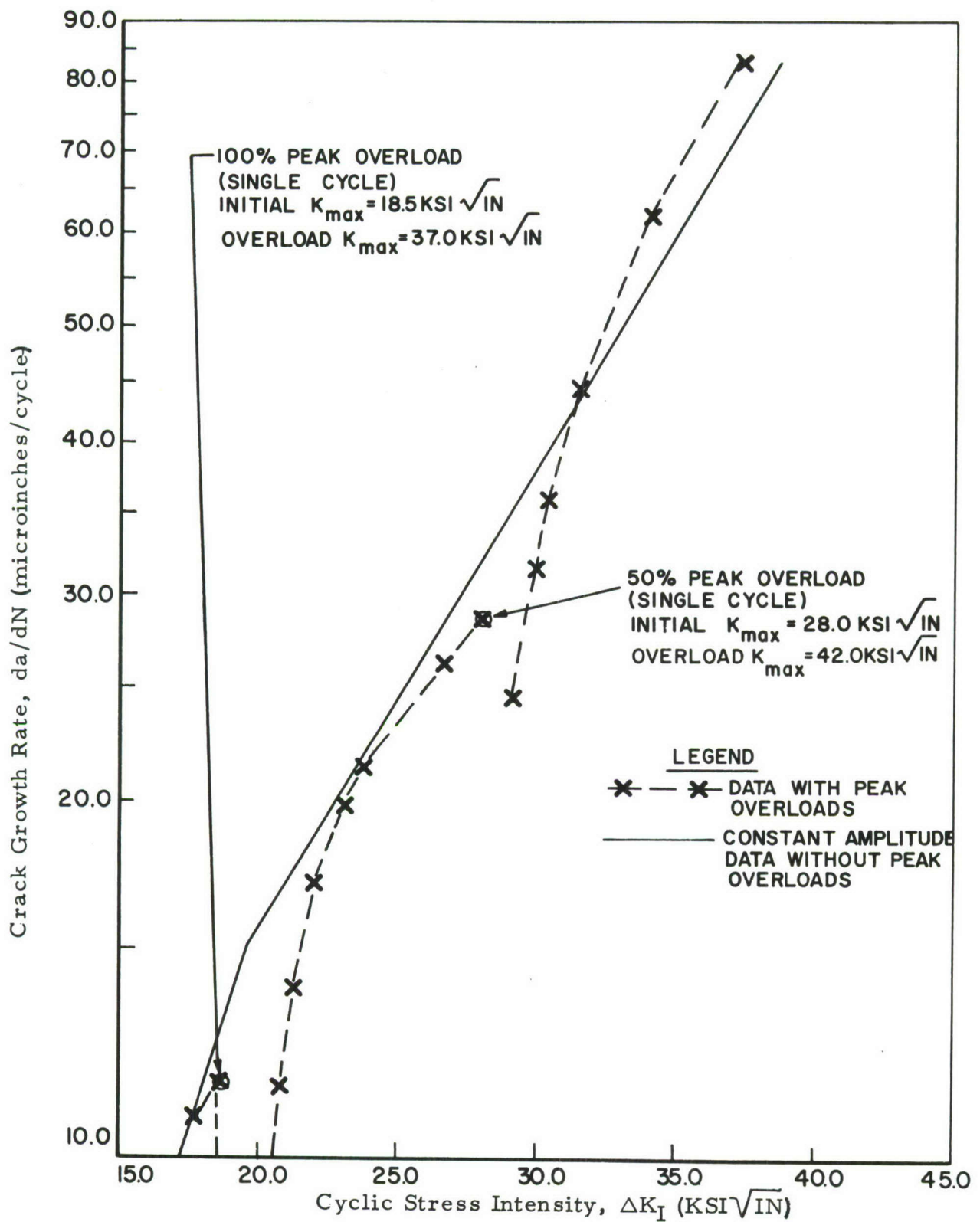
Figure 18. Crack Growth Rate Versus Cyclic Stress Intensity for 100% and 50% Single-Cycle Peak Overloads (Specimen CG-1)

22
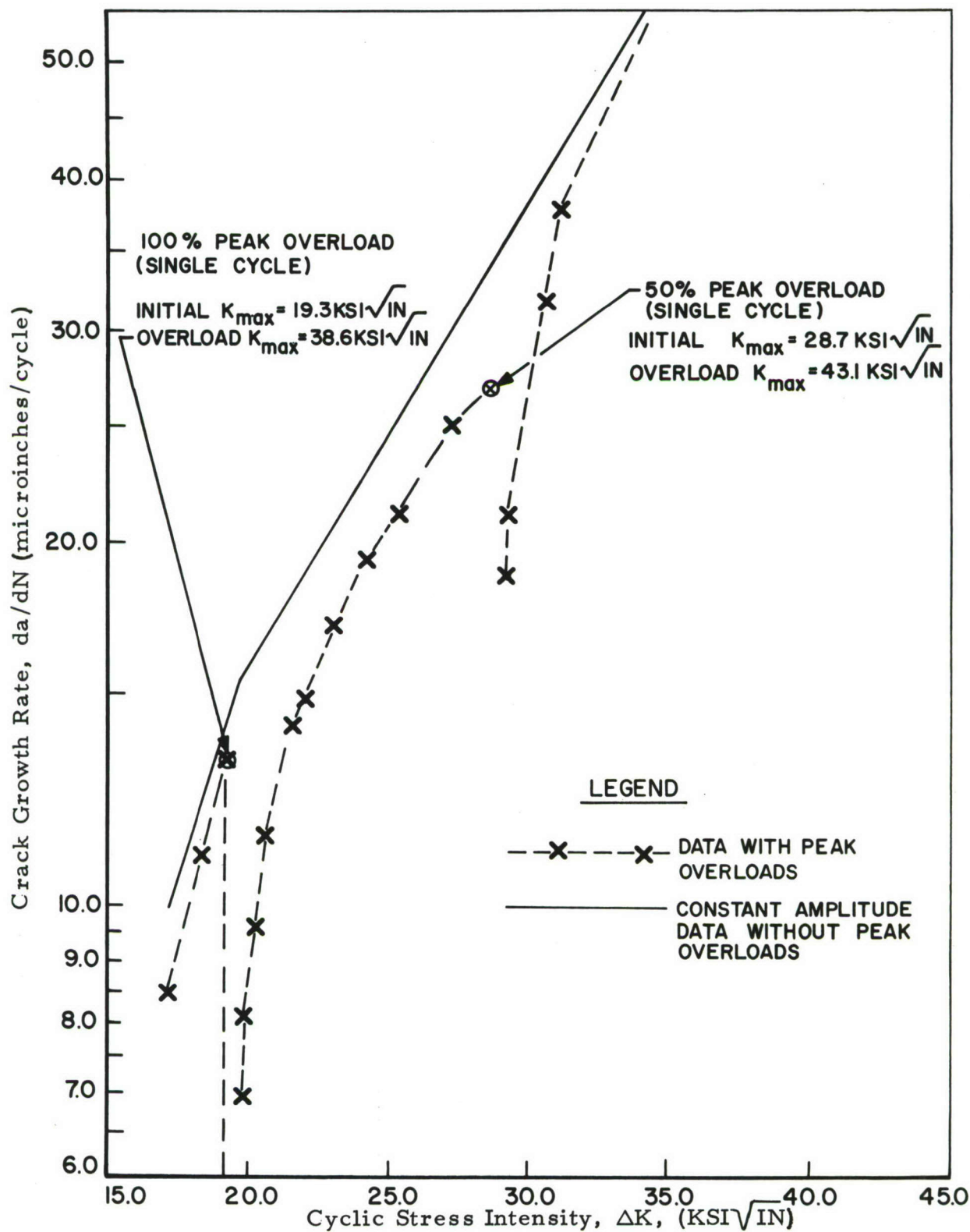
Figure 19. Crack Growth Rate Versus Cyclic Stress Intensity for 100% and 50% Single-Cycle Peak Overloads (Specimen CG-14)

TABLE III

Effects of Overload on Subsequent Crack Growth

Specimen	Overload	Affected Crack Length Increment (in Inches)*	Arrested Cycles	Total No. of Affected Cycles*
CG-14	100%	0.108	2100	10,100
	50%	0.069	-	2,500
CG-1	100%	0.096	2200	11,200
	50%	0.058	-	2,400
CG-7	70%	0.094	1000	8,200
	20%		-	-

*Crack length, as measured from the specimen's centerline, and cycles necessary to return to conditions of specimen with no peak overload. The arrested cycles were determined from the actual crack growth data, whereas the affected crack length increments and the total number of affected cycles were determined utilizing da/dN versus ΔK_I curves.

$$a_n = a_o + \sum_{i+1}^{n} C_{P_i} f(\Delta K_I)$$

or

$$(da/dN)_{O.L.} = C_P (da/dN)_{C.A.}$$

where

$$C_P = \left(\frac{R_y}{a_p - a_n}\right)^m \text{ if } a_n + R_y < a_p$$

$$C_P = 1 \text{ if } a_n + R_y \geq a_p$$

$$a_n = a_{O.L.}$$

$$(da/dN)_{C.A.} = f(\Delta K_I)$$

In order to obtain m, the data fitting constant, a loading spectrum is applied repeatedly to the same specimen. The loading spectrum may include variable amplitude loading with changing mean load and also loading frequency changes. The value of m is obtained by data correlation using the test spectra crack growth data along with constant load amplitude crack growth data. The values of m obtained from the data of this report are shown in Table IV. Although Wheeler uses m as an averaging data correlator for repeated spectrum data, the m values in Table IV were determined on an individual data point basis. Therefore, the range of instantaneous m values can be observed in the reported data as opposed to the average m value utilized by Wheeler.

Wheeler has displayed that his model gives reasonable predictions for crack growth in D6ac steel and titanium. Because the Wheeler model makes a prediction by fitting curves to previously observed data, it could not be concluded that the size of the yield zone is the factor governing retardation. The relative cyclic yield zone radius, the difference between the maximum constant load amplitude yield zone and

TABLE IV

Values of Constants for Wheeler Formula

Specimen No.	Overload	$\Delta K_{C.A.}$	C_P	m
CG-7	70%	21.0	0.55	1.02
		21.7	0.69	0.79
		22.3	0.91	0.20
CG-1	100%	20.5	0.58	0.56
		20.7	0.69	0.39
		21.2	0.81	0.25
		21.9	0.92	0.09
	50%	29.1	0.71	0.67
		29.9	0.86	0.33
		30.5	0.94	0.16
CG-14	100%	19.8	0.45	0.71
		20.3	0.61	0.47
		20.6	0.70	0.34
		21.6	0.78	0.27
	50%	29.2	0.55	1.06
		29.4	0.59	0.97
		30.6	0.79	0.48

the maximum yield zone at the time of overload, are presented in Table V.
The values of relative cyclic yield zone radius were determined by first
considering the plane strain yield zone radius formed at the tip of a
crack with a non-cyclic tensile load. Irwin (Reference 10) has determined
this non-cyclic yield zone radius to be given by:

$$r_y = (\pi/6) \cdot (K_I/\sigma_{y.s.})^2$$

The cyclic yield zone radius has been shown by Hahn, et al (Reference 11) to be considerably smaller than the non-cyclic yield zone.
These investigators have observed that the cyclic yield zone was one-fifth the size of the non-cyclic yield zone for Fe-3 Si steel using sectioning
and etching techniques. Therefore, whereas the relative difference in

non-cyclic yield zone radius is $\dfrac{\pi}{6} \left[\left(\dfrac{K_{O.L.}}{\sigma_{y.s.}} \right)^2 - \left(\dfrac{K_{C.A.}}{\sigma_{y.s.}} \right)^2 \right]$

the relative cyclic yield zone is taken in this report (in the absence of
other identifications) to be

$$\Delta r_y = (1/5) \left(\frac{\pi}{6} \right) \left[\left(\frac{K_{O.L.}}{\sigma_{y.s.}} \right)^2 - \left(\frac{K_{C.A.}}{\sigma_{y.s.}} \right)^2 \right]$$

The relative cyclic yield zone radius is considerably smaller than
the affected crack length increments presented in Table III.

The Elber concept of crack closure is based on the plastic deforma-
tion left in the wake of an overload fatigue crack as the crack grows
through the overload yield zone. Elber contends that when the crack is
unloaded the deformed material in the vicinity of the crack tip (commonly
referred to as stretch zones) goes into compression and allows the crack
to remain partially open, reducing the effective crack opening displacement

and ΔK. Since retarded crack growth was observed after the crack had exited the yield zone, it could be said that crack closure also influences cracking behavior after the crack has grown through the yield zone. The Elber crack propagation formula is as follows:

TABLE V

Relative Cyclic Yield Zone Radius After Overload

Specimen	Overload	Δr_y (inches)
CG-7	70%	0.0038
	20%	0.0020
CG-1	100%	0.0059
	100%	0.0056
CG-14	100%	0.0064
	50%	0.0059

$$da/dN = C(\Delta K \text{ eff.})^n$$

$$= C(U\Delta K_I)^n$$

where $U = \dfrac{\sigma_{max} - \sigma_{OP}}{\sigma_{max} - \sigma_{min}}$

The physical appearance (stretch zones) of specimen fracture surfaces from this program were hypothesized by the Elber concept. The Elber concept of crack closure has also been corroborated by von Euw, et al (Reference 12) for 2024-T3 aluminum alloy. Although the concept appears to be sound, it is very difficult to measure crack opening displacements near the crack tip.

Stretch zones have been noted by several investigators (Reference 13) who have attributed them to the extreme abrasive rubbing together of fracture surfaces. Fatigue striations which are usually apparent with electron fractography are obliterated in the stretch zones.

28

These zones appeared on all overloaded fracture surfaces except at the location of the 20% overload which did not affect the fatigue cracking rate. The stretch zones observed in specimen CG-14 are shown in Figure 20. These zones are followed by either striations or dimples. The lengths of stretch zones associated with overloads, as measured at the center of specimen thicknesses, are presented in Table VI. The lengths of stretch zones increased with increase in percentage of overload and were smaller than the values of relative cyclic yield zone radii as shown in Table V.

TABLE VI

Stretch Zone Length After Overload

Specimen	Overload	Approximate Stretch Zone Length (inches)
CG-7	70%	0.0004
	20%	not visible at 125X
CG-1	100%	0.0018
	50%	0.0012
CG-14	100%	0.0024
	50%	0.0016
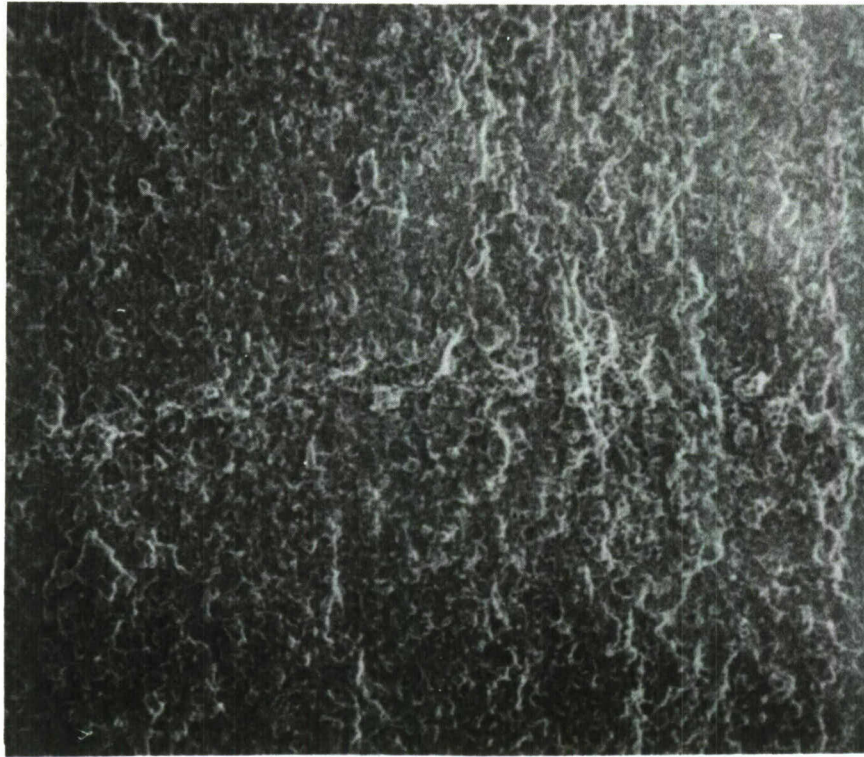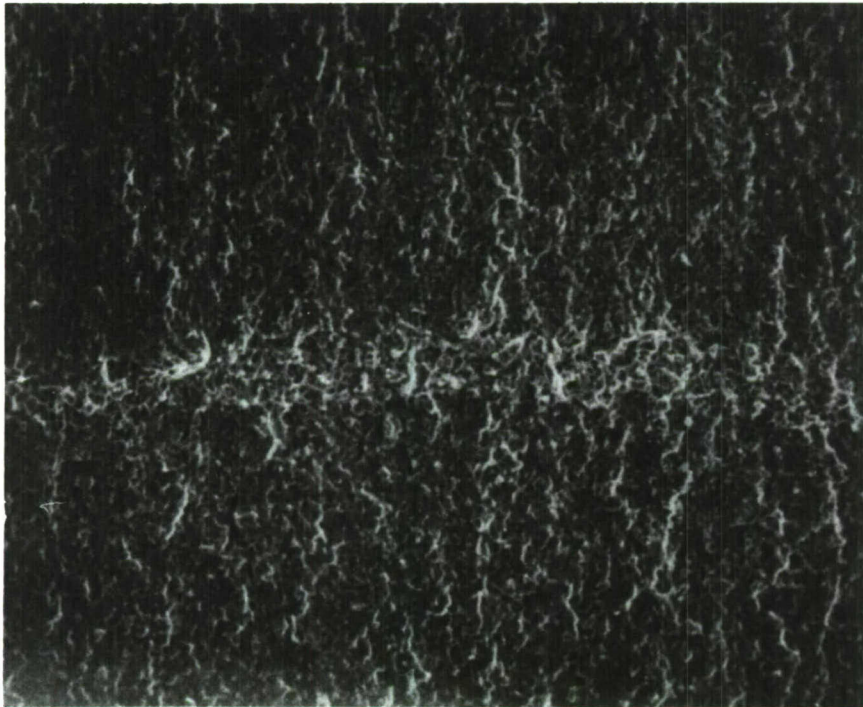
Figure 20. Overload Stretch Zones (125X)

Top: 50% Overload (Specimen CG-14); Bottom: 100% Overload (Specimen CG-14)

30

RECOVERY MODEL FOR RETARDED CRACK GROWTH

Since the design of future high performance aircraft will have to consist of some crack growth logic, it is imperative that a siutable model of crack growth due to variable amplitude loading be available. The following development may be useful for the analysis of retarded crack growth.

An approach is taken that considers the recovery of the cracking rate after overload with respect to a stable constant load amplitude cracking condition. The following basic equation is utilized:

$$(da/dN)_{O.L.} = Z \left(\frac{da}{dN} \right)_{C.A.} \tag{1}$$

where $0 \leq Z \leq 1$. Z is termed the recovery factor.

In order to determine if the recovery factor does vary with the percent overload or the $\Delta K_{C.A.}$, the recovery factors for various cyclic intensity factors are plotted in Figure 21. This figure displays a family of approximately linear relationships between Z and $\Delta K_{C.A.}$

$$Z = q\Delta K_{C.A.} + Z_o \tag{2}$$

Lines were fitted to the data points in Figure 21 using a linear least squares technique. Observing Figure 21, it was determined that $q = f(\%O.L.)$. When plotting q versus %O.L. there seemed to be a parabolic relationship (see Figure 22). The value of q can now be obtained from Figure 22. Z_o can be determined by the following relationship:

$$Z_o = Z_i - q(\Delta K_{C.A.})_i$$

where

Z_i and $(\Delta K_{C.A.})_i$ are any simultaneous recovery factor and constant amplitude cyclic stress intensity under the influence of the overload in question.

31
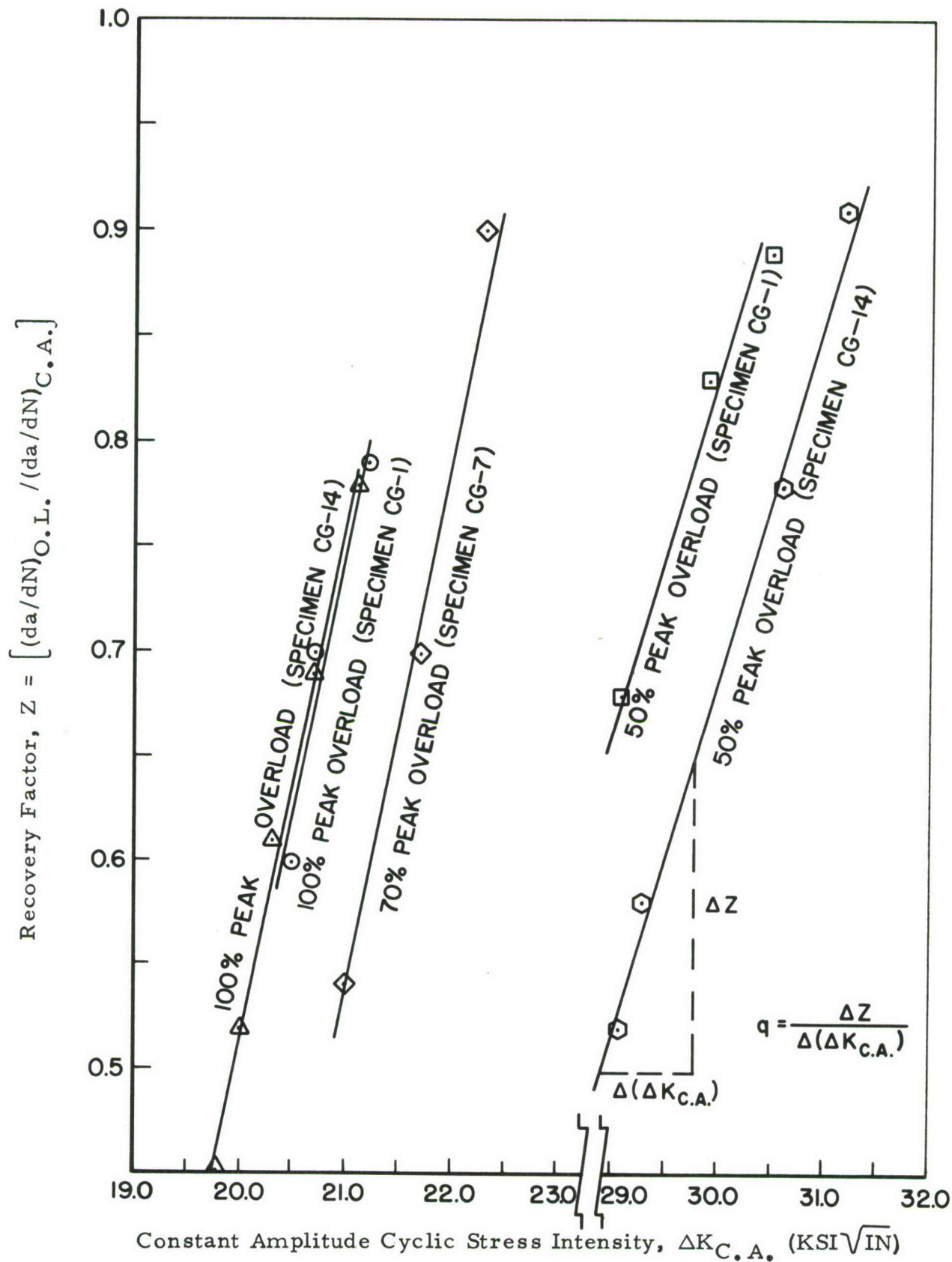
Figure 21. Recovery Factor Versus $\Delta K_{C.A.}$

32
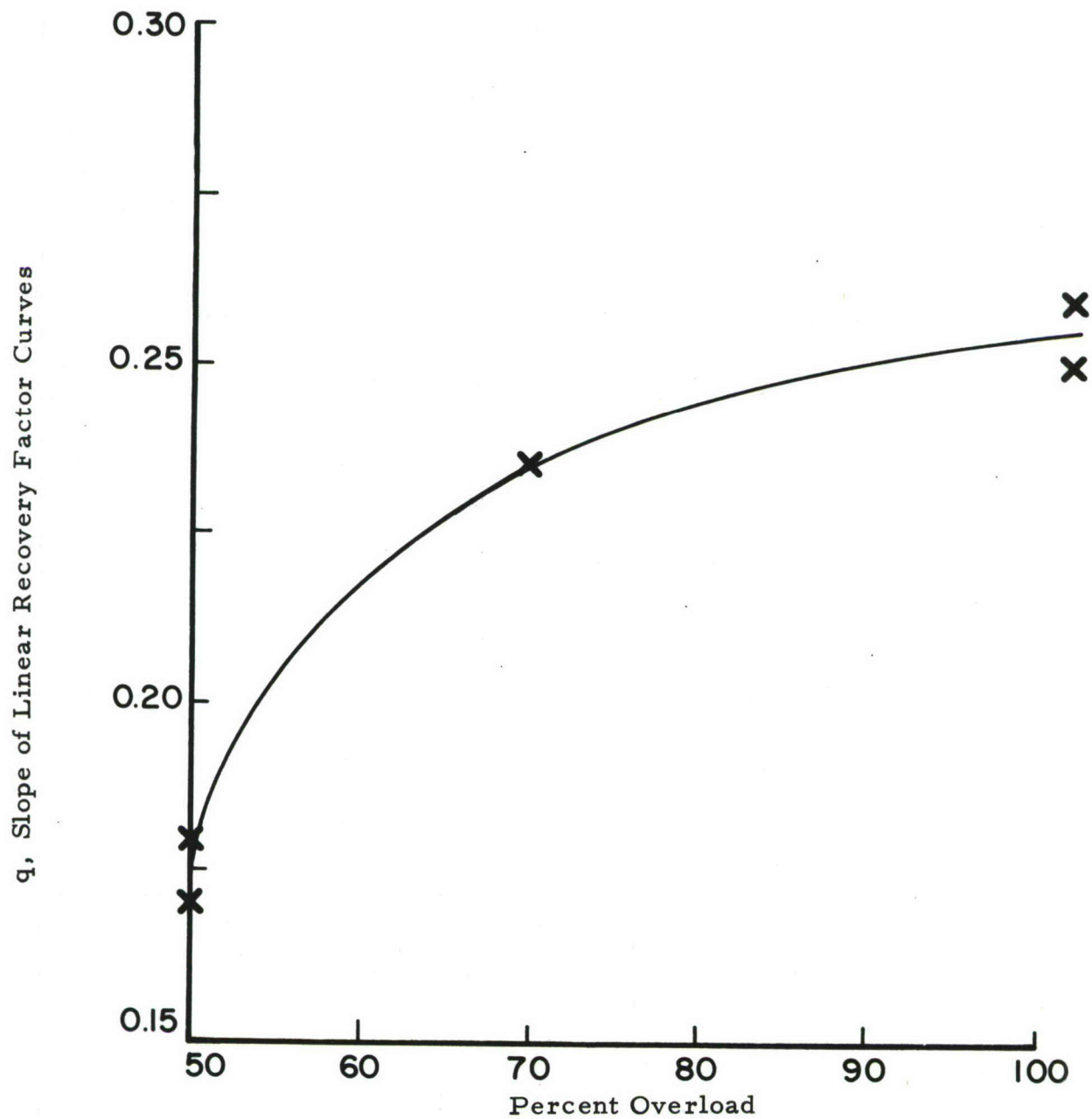
Figure 22. Percent Overload Versus the Slope of the Linear Recovery Factor Curve

33

The values of q and Z_o obtained in this report are presented in Table VII.

TABLE VII

Values of Constants for Equation 1

Specimen No.	Overload	q	Z_o
CG-14	100%	0.259	-4.668
CG-1		0.250	-4.503
CG-7	70%	0.236	-4.408
CG-1	50%	0.179	-4.540
CG-14		0.169	-4.381

When extrapolating the lines in Figure 21 to $Z = 0.0$ it was found that the $\Delta K_{C.A.}$ intercept was approximately the actual value of $\Delta K_{C.A.}$ when the overload was applied (see Table VIII). Slightly lower values of $\Delta K_{C.A.}$ were intercepted from the curves than the actual applied $\Delta K_{C.A.}$ for the 50% overloads. This is to be expected since the 50% overloads did not display crack arrest ($Z = 0.0$).

TABLE VIII

Actual and Extrapolated Values of $\Delta K_{C.A.}$

Specimen No.	Overload	Actual $\Delta K_{C.A.}$ (KSI IN)	Extrapolated $\Delta K_{C.A.}$ (KSI IN)
CG-14	100%	19.3	18.1
CG-1		18.5	18.1
CG-7	70%	18.5	18.7
CG-1	50%	28.0	25.1
CG-14		28.7	26.0

The recovery approach just presented indicates that the recovery of an overloaded fatigue crack depends upon the percentage of overload applied. The parameters necessary for computations in this approach are easily obtained. However, when implementing Equation (1) and Equation (2), it must be considered that these equations were developed (1) for the application of identical constant amplitude loading before and after each overload; (2) for cases of $0.95 > Z > 0.45$; (3) when the higher percentages of overload occurred at low $\Delta K_{C.A.}$ values and when the lower percentages of overload occurred at high $\Delta K_{C.A.}$ values; and (4) when overloads were applied far enough apart in the specimens so that there were no interacting effects.

SUMMARY

Fatigue cracks were propagated into several specimens machined from the mill annealed Ti-6Al-4V sheet while utilizing constant amplitude loading parameters. The data obtained agreed with constant load amplitude crack growth data in the literature. Other specimens prestrained to 2.41%, 3.85%, 6.10%, 7.00%, and 10.00% plastic strain showed that rather than contributing to the retardation of growth rates after overload, strain hardening mechanisms accelerate crack growth rates. Another group of specimens, which was not prestrained, received 20%, 50%, 70%, and 100% single-cycle peak overloads with the results being: (1) no effect on crack growth rates with 20% overload; (2) crack arrest following 70% and 100% overload; (3) subsequent crack retardation after crack arrest for 70% and 100% overload; and (4) retardation but no crack arrest following overload application for 50% overload. The percentage of overload was an indicator of the amount of subsequent retardation. Additionally, the relative plane strain cyclic yield zones were not an accurate indication of retardation. The appearance of stretch zones on the specimens' fracture surfaces were in agreement with the Elber concept of crack closure.

A linear empirical relationship was developed based on the recovery of the cracking rate after overload with respect to the stable constant load amplitude cracking condition. The basic equation used in this development was:

$$(da/dN)_{O.L.} = Z(da/dN)_{C.A.}$$

The recovery factor, Z, displayed a linear relationship with $\Delta K_{C.A.}$ for the data presented in this report.

Although linear recovery was considered solely for the application of identical constant amplitude loading before and after each overload,

it is speculated that recovery analysis would pertain to a change of amplitude and/or mean loading after overload. The slope of the recovery factor versus $\Delta K_{C.A.}$ might either increase or decrease with the relationship of the maximum stress intensity at the time of overload with respect to the maximum stress intensity in the constant load amplitude pattern after overload. This suggests that the maximum stress intensity before, during, and after overload may play a part in crack retardation and recovery.

The data in this report were developed so that there would be no interacting effects between applied overloads. Recovery analysis could possibly also be favorable in the case of multiple consecutive overloads. Tests of this type must be performed and a cumulative damage technique utilized to confirm this statement. However, when this situation approaches high amplitude-low cycle fatigue conditions, extensive non-localized plastic yielding may negate the analysis.

RECOMMENDATIONS

The computerization of recovery analysis for spectrum crack growth predictions is considered feasible. If so, more data than the limited quantity presented in this report is necessary for the determination of constants q and Z_o. The spectrum would be separated into peak overload, alternating overload, constant load amplitude, and other primary influences on crack growth. Recovery analysis could be used with a cumulative linear technique for crack growth predictions in peak overload segments of the spectrum.

Perhaps a more practical use of recovery analysis would be its utilization for material evaluation and the selection of materials. The method could be used to compare the retardation of crack growth in several materials.

It is recommended that further investigation be made in the region of $Z < 0.45$, although extrapolation of lines fitted to the data in this report to $Z = 0.0$ shows recovery for 100% and 70% overloads to remain linear. A look at other high strength materials in addition to Ti-6Al-4V is also necessary to demonstrate that linear recovery is not an exclusive trait of this alloy.

REFERENCES

1. Paris, P. and F. Erdogan, "A Critical Analysis of Crack Propagation Laws," Journal of Basic Engineering, December 1963, pp. 528-534.

2. Forman, et al, "Numerical Analysis of Crack Propagation in Cyclic-Loaded Structures," ASTM Annual Meeting, Paper No. 66, WA/Met.4, 1966.

3. Schijve, J. and P. deRijk, "The Effect of Ground-to-Air Cycles on the Fatigue Crack Propagation in 2024-T3 Alclad Sheet Material," NLR, TRM. 2148, Amsterdam, July 1966.

4. Srawley, et al, On the Sharpness of Cracks Compared with Wells' COD, NASA TMX-52904, September 1970.

5. Elber, W., "Fatigue Crack Closure Under Cyclic Tension," Engineering Fracture Mechanics, 1970, pp. 37-45.

6. Wheeler, O., Crack Growth Under Spectrum Loading, General Dynamics Report FZM-5602, 30 June 1970.

7. Paris, P. and G. Shi, "Stress Analysis of Cracks," Fracture Toughness Testing and Its Applications, ASTM STP 381, June 1964, p. 33.

8. Plane Strain Crack Toughness Testing of High Strength Metallic Materials, ASTM STP 410, December 1966, pp. 10-11.

9. Amateau, M., F-15 Ti-6Al-6V-2Sn and Ti-6Al-4V Crack Propagation Program, Third Interim Report, Aerospace Corporation, April 1971.

10. Irwin, G., "Relation of Crack Toughness Measurements to Practical Applications," Welding Journal Research Supplement, November 1962.

11. Hahn, et al, Local Yielding Attending Fatigue Crack Growth, ARL 71-0234, November 1971.

12. von Euw, E., et al, "Delay Effects in Fatigue Crack Propagation," unpublished work, work accomplished through National Science Foundation Grant GK-2992.

13. McMillan, J. and R. Hertzberg, "Application of Electron Fractography to Fatigue Studies," Electron Fractography, ASTM STP 436, pp. 89-123.

DOCUMENT CONTROL DATA - R&D

(Security classification of title, body of abstract and indexing annotation must be entered when the overall report is classified)

1. ORIGINATING ACTIVITY *(Corporate author)*	2a. REPORT SECURITY CLASSIFICATION
University of Dayton Research Institute 300 College Park Avenue Dayton, Ohio 45409	Unclassified
	2b. GROUP

3. REPORT TITLE

FATIGUE CRACK GROWTH RETARDATION AFTER SINGLE-CYCLE PEAK OVERLOAD IN Ti-6Al-4V TITANIUM ALLOY

4. DESCRIPTIVE NOTES *(Type of report and inclusive dates)*

Final Report (April 1971 to December 1971)

5. AUTHOR(S) *(Last name, first name, initial)*

Jones, Raymond E.

6. REPORT DATE	7a. TOTAL NO. OF PAGES	7b. NO. OF REFS
April 1972	40	13

8a. CONTRACT OR GRANT NO. F33615-71-C-1054	9a. ORIGINATOR'S REPORT NUMBER(S)
b. PROJECT NO. 7381	
c. Task No. 738106	9b. OTHER REPORT NO(S) *(Any other numbers that may be assigned this report)* AFML-TR-72-163
d.	

10. AVAILABILITY/LIMITATION NOTICES

Approved for public release; distribution unlimited.

11. SUPPLEMENTARY NOTES	12. SPONSORING MILITARY ACTIVITY
	Air Force Materials Laboratory Air Force Systems Command Wright-Patterson AFB, Ohio 45433

13. ABSTRACT

Fatigue crack growth after single-cycle peak overload was investigated in Ti-6Al-4V sheet. Strain hardening was determined not to be the major controlling mechanism retarding crack growth after peak overload, but instead, strain hardening slightly accelerated crack growth for the case when strain hardening was induced prior to crack initiation. Crack growth after peak overload was characterized by: (1) no effect after 20 percent overload (a 20 percent increase in maximum stress intensity); (2) crack arrest immediately following 70 and 100 percent overloads; (3) subsequent retarded crack growth rates after 70 and 100 percent overloads; and (4) retardation but no arrest following 50 percent overload. The Wheeler model of crack growth retardation was discussed and shown not to predict instantaneous retarded growth rates. The physical appearance of post-test fracture surfaces were as hypothesized by the Elber concept of crack closure after overload. The recovery of an overloaded crack was linear with respect to the constant load amplitude cyclic stress intensity.

DD FORM 1473
1 JAN 64

14. KEY WORDS	LINK A		LINK B		LINK C	
	ROLE	WT	ROLE	WT	ROLE	WT
Titanium Alloy Ti-6Al-4V Sheet Peak Overload Strain Hardening Fatigue Crack Growth Retardation						

INSTRUCTIONS

1. ORIGINATING ACTIVITY: Enter the name and address of the contractor, subcontractor, grantee, Department of Defense activity or other organization (*corporate author*) issuing the report.

2a. REPORT SECURITY CLASSIFICATION: Enter the overall security classification of the report. Indicate whether "Restricted Data" is included. Marking is to be in accordance with appropriate security regulations.

2b. GROUP: Automatic downgrading is specified in DoD Directive 5200.10 and Armed Forces Industrial Manual. Enter the group number. Also, when applicable, show that optional markings have been used for Group 3 and Group 4 as authorized.

3. REPORT TITLE: Enter the complete report title in all capital letters. Titles in all cases should be unclassified. If a meaningful title cannot be selected without classification, show title classification in all capitals in parenthesis immediately following the title.

4. DESCRIPTIVE NOTES: If appropriate, enter the type of report, e.g., interim, progress, summary, annual, or final. Give the inclusive dates when a specific reporting period is covered.

5. AUTHOR(S): Enter the name(s) of author(s) as shown on or in the report. Enter last name, first name, middle initial. If military, show rank and branch of service. The name of the principal author is an absolute minimum requirement.

6. REPORT DATE: Enter the date of the report as day, month, year; or month, year. If more than one date appears on the report, use date of publication.

7a. TOTAL NUMBER OF PAGES: The total page count should follow normal pagination procedures, i.e., enter the number of pages containing information.

7b. NUMBER OF REFERENCES: Enter the total number of references cited in the report.

8a. CONTRACT OR GRANT NUMBER: If appropriate, enter the applicable number of the contract or grant under which the report was written.

8b, 8c, & 8d. PROJECT NUMBER: Enter the appropriate military department identification, such as project number, subproject number, system numbers, task number, etc.

9a. ORIGINATOR'S REPORT NUMBER(S): Enter the official report number by which the document will be identified and controlled by the originating activity. This number must be unique to this report.

9b. OTHER REPORT NUMBER(S): If the report has been assigned any other report numbers (*either by the originator or by the sponsor*), also enter this number(s).

10. AVAILABILITY/LIMITATION NOTICES: Enter any limitations on further dissemination of the report, other than those imposed by security classification, using standard statements such as:

(1) "Qualified requesters may obtain copies of this report from DDC."

(2) "Foreign announcement and dissemination of this report by DDC is not authorized."

(3) "U. S. Government agencies may obtain copies of this report directly from DDC. Other qualified DDC users shall request through

_____."

(4) "U. S. military agencies may obtain copies of this report directly from DDC. Other qualified users shall request through

_____."

(5) "All distribution of this report is controlled. Qualified DDC users shall request through

_____."

If the report has been furnished to the Office of Technical Services, Department of Commerce, for sale to the public, indicate this fact and enter the price, if known.

11. SUPPLEMENTARY NOTES: Use for additional explanatory notes.

12. SPONSORING MILITARY ACTIVITY: Enter the name of the departmental project office or laboratory sponsoring (*paying for*) the research and development. Include address.

13. ABSTRACT: Enter an abstract giving a brief and factual summary of the document indicative of the report, even though it may also appear elsewhere in the body of the technical report. If additional space is required, a continuation sheet shall be attached.

It is highly desirable that the abstract of classified reports be unclassified. Each paragraph of the abstract shall end with an indication of the military security classification of the information in the paragraph, represented as (*TS*), (*S*), (*C*), or (*U*).

There is no limitation on the length of the abstract. However, the suggested length is from 150 to 225 words.

14. KEY WORDS: Key words are technically meaningful terms or short phrases that characterize a report and may be used as index entries for cataloging the report. Key words must be selected so that no security classification is required. Identifiers, such as equipment model designation, trade name, military project code name, geographic location, may be used as key words but will be followed by an indication of technical context. The assignment of links, rules, and weights is optional.